Catalysis Communications 88 (2017) 85–89

Contents lists available at ScienceDirect

Catalysis Communications

journal homepage: www.elsevier.com/locate/catcom

Short communication

Tuning component enrichment in amino acid functionalized (organo)silicas

Jeroen Lauwaert [a,1], Judith Ouwehand [b], Jeriffa De Clercq [c], Pegie Cool [d], Pascal Van Der Voort [b], Joris W. Thybaut [a,*]

[a] Ghent University, Department of Chemical Technology, Laboratory for Chemical Technology, Tech Lane Ghent Science Park, Campus A 914, 9052 Ghent, Belgium
[b] Ghent University, Department of Inorganic and Physical Chemistry, Center for Ordered Materials, Organometallics & Catalysis, Krijgslaan 281 (S3), 9000 Ghent, Belgium
[c] Ghent University, Department of Chemical Technology, Industrial Catalysis and Adsorption Technology, Valentin Vaerwyckweg 1, 9000 Ghent, Belgium
[d] University of Antwerp, Department of Chemistry, Laboratory of Adsorption and Catalysis, Universiteitsplein 1, 2610 Wilrijk, Belgium

ARTICLE INFO

Article history:
Received 4 July 2016
Received in revised form 4 October 2016
Accepted 5 October 2016
Available online 6 October 2016

Keywords:
Heterogeneous catalysis
Mesoporous materials
Click chemistry
Amino acids
Aldol reactions

ABSTRACT

A straightforward procedure to synthesize cysteine functionalized materials with tailored support properties has been developed. It allows tuning the hydrophobicity of the material via the incorporation of aliphatics, aromatics or silica in the framework structure. The aldol condensation of 4-nitrobenzaldehyde and acetone, as a probe reaction for the catalytic activity of the produced materials, exhibited a remarkable interplay between the reactant, solvent, traces of water and support hydrophobicity. A selective enrichment in the catalyst pores of specific bulk phase molecules is believed to be the key to achieve the targeted catalyst performance.

1. Introduction

Since the development of mesoporous silica materials, such as the MCM and SBA families [1,2], research on these materials has ever been increasing. They are characterized by large pore sizes, i.e., between 2 and 50 nm and large surface areas, often exceeding 1000 m^2/g. Moreover, the functionality of silica materials can easily be manipulated by incorporation of active sites in the walls (co-condensation) or by anchoring active species on the surface (post-functionalization). As a result, mesoporous silica materials exhibit promising performances in many applications including adsorption [3,4], chromatography [5,6], electronics [7,8], drug delivery [9,10] and catalysis [11,12]. In the framework of catalysis, an interesting research field is situated in the use of aminated silica materials to catalyze carbon-carbon coupling reactions [13–22]. These reactions are widely used in the pharmaceutical industry and fine chemicals production [23]. Moreover, a bright future in the valorization of biomass-based resources has been forecasted for these reactions [24,25]. However, mesoporous silica materials exhibit a limited hydrothermal stability, which is often related to the hydrolysis of Si-O-Si bonds [26,27]. Hence, the water tolerance of these materials should be enhanced in order to further broaden their scope of application.

In 1999, three research groups, independent from one another, incorporated organic groups in the pore walls through the condensation of bridged organobissilanes, with the general formula $(R'O)_3$-Si-R-Si-$(OR')_3$, in the presence of a surfactant [28–30]. The presence of the organic moieties specifically results in periodic mesoporous organosilicas (PMOs), which have a more hydrophobic character compared to the original silica materials. It turns the PMOs into materials which are comparatively more robust in an aqueous environment [31]. Originally, only a limited number of organobissilanes (methane, ethane, ethene and benzene bissilanes) were used. Nowadays, a wide variety is available, providing opportunities to tune the hydrophobicity of the organosilica materials. Moreover, these organobissilanes allow the incorporation of a more extended range of functional groups in the materials, either by the direct introduction via the organobissilanes or by the post-modification of the organic moieties incorporated in the pore walls [32].

In this work, the wide variety of organo(bis)silanes is used to probe the selective enrichment of reactant molecules in amino acid functionalized catalysts and, consequently, optimize the catalytic performance in different environments. A catalyst library comprising different cysteine functionalized materials is prepared and the effect of the incorporation of different organic moieties is investigated in the aldol reaction of acetone with 4-nitrobenzaldehyde. Additionally, the ability of the materials to cope with traces of water in the reaction mixture is studied.

* Corresponding author.
E-mail address: Joris.Thybaut@UGent.be (J.W. Thybaut).
[1] Present address: Ghent University, Department of Chemical Technology, Industrial Catalysis and Adsorption Technology, Valentin Vaerwyckweg 1, 9000 Ghent, Belgium.

http://dx.doi.org/10.1016/j.catcom.2016.10.001

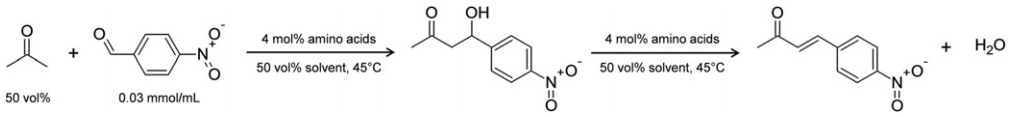

Scheme 1. Aldol condensation of acetone and 4-nitrobenzaldehyde towards the primary aldol product, 4-hydroxy-4-(4-nitrophenyl)-3-buten-2-one, and the secondary ketone product, 4-(4-nitrophenyl)-3-buten-2-one.

2. Experimental procedures

2.1. Catalyst synthesis

Three catalysts have been synthesized in the present work. Two had hydrophobic organosilica supports, i.e., catalyst E, which was synthesized using 1,2-bis(triethoxysilyl)ethane (BTEE, 97%, ABCR) and catalyst B synthesized using 1,4-bis(triethoxysilyl)benzene (BTEB, 95%, ABCR). The third one had a hydrophilic silica support, i.e., catalyst S synthesized using tetraethyl orthosilicate (TEOS, 98%, ABCR). 1 to 10 mol% vinyltriethoxysilane (VTES, 98% ABCR) was also included during the synthesis to allow post-functionalization with cysteine. A final amino acid site density in the range between 0.06 and 0.07 mmol/g was aimed at because at higher site densities intermolecular interactions between amino acids on different linkers may lead to a significant decrease of the turnover frequency (TOF) [33].

The supports were synthesized according to the following recipe: about 3 g Brij S10 ($C_{18}H_{37}(OCH_2CH_2)_nOH$, n~10, Sigma-Aldrich) was dissolved in a mixture of 138 mL demineralized water and 10 mL 12.1 M hydrochloric acid (HCl, ACS grade reagent, Sigma-Aldrich). The mixture was stirred for 4 h at 50 °C in order to form micelles. Afterwards, 2.5×10^{-2} mol of Si atoms in the form of TEOS or one of the organobissilanes and VTES was added and the mixture was stirred at 50 °C for 24 h. Subsequently, the magnetic stir bar was removed and the mixture was heated to 90 °C for 24 h. The resulting solid was separated from the mixture by filtration and, subsequently, washed three times by stirring at 80 °C for 24 h in a 98 vol% ethanol (96%, Fiers) – 2 vol% HCl mixture followed by filtration. The material was dried overnight under vacuum at 100 °C.

Afterwards, the supports were functionalized. 2 g L-cysteine (99 + %, Acros) and 1 g 2-hydroxy-4′-(2-hydroxyethoxy)-2-methylpropiophenone (98%, Sigma-Aldrich) were dissolved in 50 mL distilled water, 1 g of the solid material was added and the mixture was stirred for 24 h in a Metalight Classic UV reactor (360 nm). The material was recovered by filtration and subsequently washed several times with demineralized water by stirring for 3 h at 40 °C. Finally, the material was dried under vacuum with heating to 100 °C and stored in an inert atmosphere.

2.2. Catalyst characterization

Nitrogen adsorption-desorption measurements were carried out at 77 K using a Micromeritics Tristar II 3020 apparatus. Samples were degassed at 120 °C for 17 h prior to measurement. The specific surface area and pore volume were determined using the Brunauer-Emmett-Teller method. The total pore volumes and pore sizes were calculated using the Broekhoff-de Boer method with the Frenkel-Halsey-Hill modification. The pore ordering of the materials was determined using X-ray diffraction (XRD) patterns which were measured on a Thermo Scientific ARL X'TRA X-ray diffractometer. In order to qualitatively confirm the presence of the functional groups Diffuse Reflectance Infrared Fourier Transform (DRIFT) spectroscopy was performed on a Nicolet 6700 spectrometer of Thermo Scientific with a nitrogen cooled MCT-A detector using a Graseby Specac diffuse reactant cell, operating in vacuum at 120 °C. The amino acid site density was determined using elemental (CHNS) analysis. These experiments were performed on a Thermo Flash 2000 elemental analyzer. 4-nitrobenzaldehyde adsorption capacities were determined by adding 0.3 g of support material in 5 mL of acetone (50 vol%), *n*-hexane (50 vol%) and 4-nitrobenzaldehde (0.003 mmol/mL). The mixture was stirred for 3 h at room temperature after which the decrease in the liquid phase 4-nitrobenzaldehyde concentration was determined via reversed-phase HPLC (Agilent 1100).

2.3. Catalyst performance testing

The activity of each catalyst was assessed in the aldol condensation of acetone (99.6%, Acros) and 4-nitrobenzaldehyde (99%, Acros), see Scheme 1, according to the procedure as published before [33]. The experiments were performed initially in the presence of a nonpolar aprotic solvent, i.e., *n*-hexane and, subsequently, in the presence of the same solvent including 1 vol% of water. Such an amount significantly exceeds that which can remain in the catalyst pores after synthesis. All data were obtained at differential conditions, meaning that the conversion depended linearly on the batch time and the TOF could be determined from the slope of the observed straight line.

3. Results and discussion

3.1. Catalyst characterization

Three supported amino acid catalysts have been synthesized in the present work, i.e., catalyst E containing ethane bridges, catalyst B containing benzene bridges and a hydrophilic silica material, catalyst S.

The specific BET surface areas, average pore sizes and total pore volumes of the three supports and the corresponding, functionalized catalysts are listed in Table 1. The nitrogen sorption isotherms and the corresponding pore size distributions are reported in the supporting information. All supports are mesoporous with a large specific BET surface area between 870 and 970 m^2/g, an average pore size between 3.1 and 4.1 nm and a total pore volume between 0.70 and 1.08 cm^3/g. Before

Table 1
Catalyst properties determined via nitrogen adsorption-desorption measurements, X-ray diffraction and elemental analysis.

Catalyst	BET surface area (m^2/g)	Average pore diameter (nm)	Total pore volume (cm^3/g)	Unit cell width (nm)	Wall thickness (nm)	Amino acid loading (mmol/g)
Aliphatic support	928	3.7	0.94	6.7	3.0	0.00
Catalyst E	783	3.7	0.82	6.8	3.1	0.06
Aromatic support	970	3.1	0.70	6.1	3.0	0.00
Catalyst B	654	3.1	0.46	5.8	2.7	0.07
Silica support	860	4.1	1.08	6.7	2.6	0.00
Catalyst S	690	5.1	0.68	6.7	1.6	0.07

functionalization the XRD patterns of all three supports exhibit the characteristic (100), (110) and (200) reflections of a hexagonal pore ordering [2], see supporting information. After functionalization a decrease in the specific BET surface area and total pore volume of the samples, resulting from the loss in free volume and the increase in catalyst mass is observed. The XRD patterns as well as the nitrogen sorption isotherms show that the ordering of catalysts S and B has slightly degraded with a decrease in wall thickness as a result. In the case of catalyst S, the average pore diameter has even increased by 1 nm. This is ascribed to some structural degradation by the aqueous environment during functionalization and the heat generated during the thiol-ene click reaction. However, the characterization results confirm that the mesoporosity and hexagonal pore ordering of all materials is largely retained.

The DRIFT spectra of the functionalized materials exhibit a characteristic silanol peak around 3720 cm^{-1}, several bands in the range of 2800–3100 cm^{-1} originating from C-H stretches of both the support and the functional groups, a carbonyl peak at 1730 cm^{-1} and a N-H bending peak at 1615 cm^{-1}, see Fig. 1. This qualitatively confirms the presence of the amino acid functional groups. The active site concentration was determined from the nitrogen content on the catalyst as obtained by CHNS elemental analysis. All materials have an active site density of about 0.07 mmol/g, see Table 1, equivalent with an area per amino acid between 15 and 22 nm^2. Previous work on a cysteine functionalized ethylene-bridged PMO showed that such a low site density prevents intermolecular interactions between functional groups, such as hydrogen bonding or acid-base neutralization. Hence, differences in surface area can be safely discarded as a potential origin for activity differences [33].

3.2. Catalyst performance evaluation and interpretation

The synthesized materials have been used to investigate the effect of the support hydrophobicity on their aldol condensation performance for 4-nitrobenzaldehyde and acetone using 4 mol% of amino acids with respect to the concentration of 4-nitrobenzaldehyde in the reaction mixture (0.03 M). First, a 50:50 acetone/*n*-hexane mixture was used because nonpolar aprotic solvents are reported to result in better catalytic activity of acid-base pairs supported on a silica material [14]. Subsequently, the experiments were repeated with 1 vol% water present in the reaction mixture. No conversion was observed when using the unmodified support materials. The conversion curves obtained with the functionalized materials are shown in the supporting information while the TOFs are reported in Table 2. All three catalysts exhibited high selectivities towards the aldol product (> 90%).

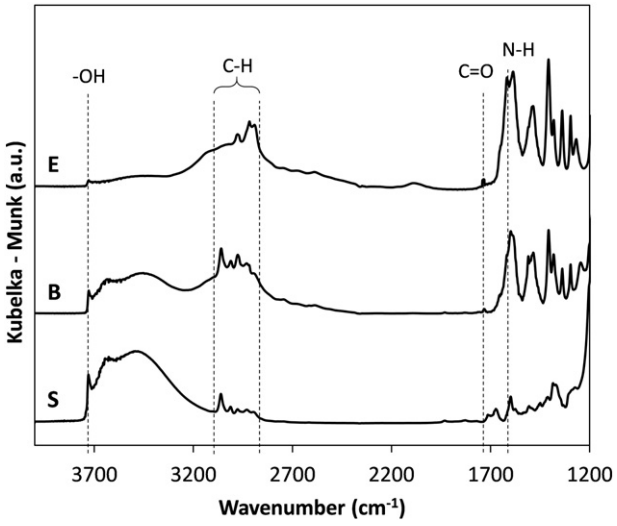

Fig. 1. DRIFT spectra of catalyst S, catalyst B and catalyst E.

Table 2
Turnover frequencies in the absence of water and in the presence of 1 vol% water obtained at 45 °C in 50 vol% acetone and 50 vol% solvent (*n*-hexane and water) using 4 mol% of amino acids with respect to the concentration of 4-nitrobenzaldehyde (0.03 mmol/mL).

Catalyst	Water free	1 vol% water
Catalyst E	$1.92 \times 10^{-4}\ s^{-1}$	$1.96 \times 10^{-4}\ s^{-1}$
Catalyst B	$1.83 \times 10^{-5}\ s^{-1}$	$1.32 \times 10^{-5}\ s^{-1}$
Catalyst S	$8.67 \times 10^{-5}\ s^{-1}$	$5.15 \times 10^{-5}\ s^{-1}$

Without adding water to the reaction mixture, the hydrophilic silica, catalyst S, exhibits a TOF of $8.67 \times 10^{-5}\ s^{-1}$, while the organosilica with an aliphatic character, catalyst E, and the organosilica with an aromatic character, catalyst B, gave rise to TOFs of $1.92 \times 10^{-4}\ s^{-1}$ and $1.83 \times 10^{-5}\ s^{-1}$, respectively. These results suggest that, at the investigated reaction conditions, a hydrophobic aliphatic support, catalyst E, has a better acetone to 4-nitrobenzaldehyde ratio inside its pores compared to the hydrophilic silica support, catalyst S, see Fig. 2. The large amount of silanols on the surface of the hydrophilic silica support can then form preferential hydrogen bonds with acetone, due to its polar character. This, in turn, results in an acetone enrichment in the pores and enhances the formation of the reactive enamine intermediate. However, this enrichment simultaneously prevents 4-nitrobenzaldehyde from efficiently reaching the enamine intermediate, resulting in a decreased TOF without leading to acetone self-condensation. The hydrophobic support with an aromatic character, catalyst B, exhibits a TOF which is about an order of magnitude lower than that obtained with the aliphatic support, catalyst E. The low activity of catalyst B could be explained by a strong 4-nitrobenzaldehyde enrichment in the pore structure originating from the 'like-likes-like' principle, see Fig. 2. This strong enrichment results in an increased direct interaction between 4-nitrobenzaldehyde and the active site, which is expected to yield inhibiting species such as an imine or an 1,3-oxazolidin-5-one [17,19,20,34], see Fig. 2. These species decrease the reactive enamine intermediate concentration and, hence, also the TOF. Adsorption experiments indicate that the aromatic support, indeed, adsorbs about an order of magnitude more 4-nitrobenzaldehyde than the aliphatic and the silica support, which is consistent with the 4-nitrobenzaldehyde enrichment and inhibition hypothesis. In short, a crucial interplay between the reactant and support hydrophobicity is deemed responsible for significant differences in concentrations inside the catalyst and in the bulk liquid. This provides opportunities to, potentially, achieve the desired catalyst performance by tuning the support properties.

In the presence of 1 vol% water, the TOF exhibited by the hydrophilic material, catalyst S, drops by about 40% to $5.15 \times 10^{-5}\ s^{-1}$ compared to that observed in the absence of water. This pronounced decrease is ascribed to the hydrophilic character of the silica allowing water to penetrate easily into the pores, see Fig. 2. The water molecules inside the pores are believed to poison the active sites, either via the formation of hydrogen bonds with the active sites or via a pronounced shift in the equilibrium from the free acid and free base towards the resulting neutralized ion pair [14]. Additionally, as a consequence of Le Chatelier's principle, an increased water concentration suppresses the formation of the reactive enamine intermediate which then also leads to a decrease of the TOF. Catalyst B exhibits a TOF of $1.32 \times 10^{-5}\ s^{-1}$ in the presence of 1 vol% water, which corresponds to a decrease of 28% compared to water free conditions. As benzene-bridged organosilicas have a rather hydrophobic character compared to the silica materials [35], water is largely repelled from the pores of catalyst B. However, the experimental data suggest that some water is still able to enter the catalyst pores, see Fig. 2. Apart from the negative effect induced by the presence of water on the TOF, as observed with catalyst S, water will suppress the

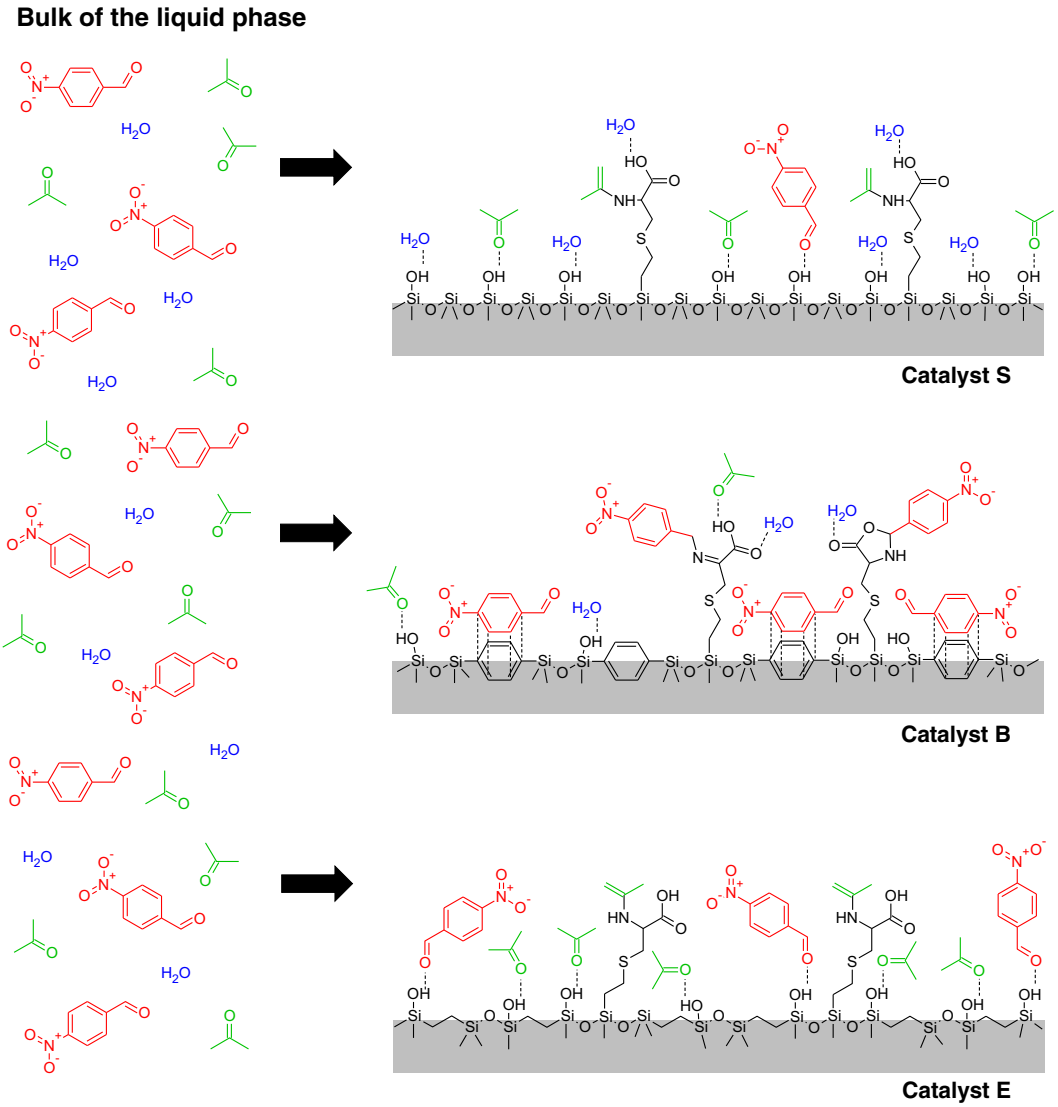

Fig. 2. Representation of the selective enrichment and the related formation of reactive enamine intermediates and inhibiting species in the pores of silica material, catalyst S, catalyst B containing benzene bridges and catalyst E containing ethane bridges.

formation of the inhibiting species originating from the direct interaction between 4-nitrobenzaldehyde and the active site [34]. Both factors allow explaining the less pronounced decrease in catalytic activity in the presence of 1 vol% water as observed on catalyst B compared to catalyst S. Finally, the aliphatic organosilica, catalyst E, fully preserves its activity in the presence of 1 vol% water. This suggests that the hydrophobic walls of the support fully impede the additional water to enter the pores and, hence, prevent poisoning of the active sites and suppression of the enamine formation. These observations nicely illustrate how, in addition to the reactant properties, also the properties of other molecules in the reaction mixture, i.e., solvents and traces, impact on the optimization of the catalyst support properties.

4. Conclusions

A straightforward synthesis procedure for cysteine functionalized (organo)silicas with an aliphatic, aromatic or silica character has been developed. Catalytic testing of the synthesized materials in the aldol condensation of 4-nitrobenzaldehyde and acetone was indicative of a crucial interplay between the reactant, solvent, traces and support properties in achieving the desired catalyst performance. An organosilica with aromatic linkers exhibited a low catalytic activity, which was attributed to a pronounced 4-nitrobenzaldehyde enrichment enhancing the formation of inhibiting species. Of the two other catalysts, i.e., an organosilica with an aliphatic character and a hydrophilic silica material, the former exhibits the highest catalytic activity. This suggests that a hydrophobic support might lead to a better acetone to 4-nitrobenzaldehyde ratio inside its pores and, hence, would be beneficial for the catalytic activity. Additionally, the hydrophilic silica material loses about 40% of its activity in the presence of a small amount of water due to poisoning of the active sites and suppression of the formation of the reactive enamine intermediate. The aromatic organosilica exhibits an activity decrease of 28% in agreement with its hydrophobic character and the suppression of the formation of inhibiting species while the aliphatic organosilica apparently fully repels water from its pores and retains its activity.

Acknowledgements

This work was supported by the European Research Council under the European Union's Seventh Framework Programme (FP7/2007-2013) through ERC grant agreement no. 615456 i-CaD, the Fund for Scientific Research Flanders (FWO) through grant number 3G006813 and the Long Term Structural Methusalem Funding by the Flemish

Government. The authors would like to thank Tom Planckaert for performing the CHNS elemental analysis, Tom Planckaert and Hannes De Pauw for XRD measurements, Jonathan De Vydt for the help with the catalyst synthesis and aldol reaction experiments and dr. Els De Canck and dr. Dolores Esquivel for the useful discussions.

References

[1] C.T. Kresge, M.E. Leonowicz, W.J. Roth, J.C. Vartuli, J.S. Beck, Nature 359 (1992) 710–712.
[2] D.Y. Zhao, J.L. Feng, Q.S. Huo, N. Melosh, G.H. Fredrickson, B.F. Chmelka, G.D. Stucky, Science 279 (1998) 548–552.
[3] A.M. Liu, K. Hidajat, S. Kawi, D.Y. Zhao, Chem. Commun. (2000) 1145–1146.
[4] J.H. Drese, S. Choi, R.P. Lively, W.J. Koros, D.J. Fauth, M.L. Gray, C.W. Jones, Adv. Funct. Mater. 19 (2009) 3821–3832.
[5] M. Grün, A.A. Kurganov, S. Schacht, F. Schuth, K.K. Unger, J. Chromatogr. A 740 (1996) 1–9.
[6] A. Kurganov, K. Unger, T. Issaeva, J. Chromatogr. A 753 (1996) 177–190.
[7] H. Miyata, T. Suzuki, A. Fukuoka, T. Sawada, M. Watanabe, T. Noma, K. Takada, T. Mukaide, K. Kuroda, Nat. Mater. 3 (2004) 651–656.
[8] B.J. Melde, B.J. Johnson, Anal. Bioanal. Chem. 398 (2010) 1565–1573.
[9] R. Mellaerts, R. Mols, J.A.G. Jammaer, C.A. Aerts, P. Annaert, J. Van Humbeeck, G. Van den Mooter, P. Augustijns, J.A. Martens, Eur. J. Pharm. Biopharm. 69 (2008) 223–230.
[10] P.P. Yang, S.L. Gai, J. Lin, Chem. Soc. Rev. 41 (2012) 3679–3698.
[11] T. Yokoi, Y. Kubota, T. Tatsumi, Appl. Catal. A Gen. 421 (2012) 14–37.
[12] L.B. Sun, X.Q. Liu, H.C. Zhou, Chem. Soc. Rev. 44 (2015) 5092–5147.
[13] J.D. Bass, A. Solovyov, A.J. Pascall, A. Katz, J. Am. Chem. Soc. 128 (2006) 3737–3747.
[14] R.K. Zeidan, S.J. Hwang, M.E. Davis, Angew. Chem.-Int. Edit. 45 (2006) 6332–6335.
[15] K.K. Sharma, R.P. Buckley, T. Asefa, Langmuir 24 (2008) 14306–14320.
[16] Y. Kubota, H. Yamaguchi, T. Yamada, S. Inagaki, Y. Sugi, T. Tatsumi, Top. Catal. 53 (2010) 492–499.
[17] K. Kandel, S.M. Althaus, C. Peeraphatdit, T. Kobayashi, B.G. Trewyn, M. Pruski, I.I. Slowing, J. Catal. 291 (2012) 63–68.
[18] N.A. Brunelli, C.W. Jones, J. Catal. 308 (2013) 60–72.
[19] K. Kandel, S.M. Althaus, C. Peeraphatdit, T. Kobayashi, B.G. Trewyn, M. Pruski, I.I. Slowing, ACS Catal. 3 (2013) 265–271.
[20] J. Lauwaert, E. De Canck, D. Esquivel, P. Van der Voort, J.W. Thybaut, G.B. Marin, Catal. Today 246 (2015) 35–45.
[21] J. Lauwaert, E.G. Moschetta, P. Van der Voort, J.W. Thybaut, C.W. Jones, G.B. Marin, J. Catal. 325 (2015) 19–25.
[22] V.E. Collier, N.C. Ellebracht, G.I. Lindy, E.G. Moschetta, C.W. Jones, ACS Catal. 6 (2016) 460–468.
[23] S. Bhaduri, D. Mukesh, Homogeneous Catalysis: Mechanisms and Industrial Applications, John Wiley & Sons, Inc., 2000
[24] J.N. Chheda, G.W. Huber, J.A. Dumesic, Angew. Chem. Int. Edit. 46 (2007) 7164–7183.
[25] J.C. Serrano-Ruiz, J.A. Dumesic, Energy Environ. Sci. 4 (2011) 83–99.
[26] K. Cassiers, T. Linssen, M. Mathieu, M. Benjelloun, K. Schrijnemakers, P. Van Der Voort, P. Cool, E.F. Vansant, Chem. Mater. 14 (2002) 2317–2324.
[27] N. Igarashi, K.A. Koyano, Y. Tanaka, S. Nakata, K. Hashimoto, T. Tatsumi, Microporous Mesoporous Mater. 59 (2003) 43–52.
[28] S. Inagaki, S. Guan, Y. Fukushima, T. Ohsuna, O. Terasaki, J. Am. Chem. Soc. 121 (1999) 9611–9614.
[29] B.J. Melde, B.T. Holland, C.F. Blanford, A. Stein, Chem. Mater. 11 (1999) 3302–3308.
[30] T. Asefa, M.J. MacLachlan, N. Coombs, G.A. Ozin, Nature 402 (1999) 867–871.
[31] D. Esquivel, C. Jimenez-Sanchidrian, F.J. Romero-Salguero, Mater. Lett. 65 (2011) 1460–1462.
[32] P. Van der Voort, D. Esquivel, E. De Canck, F. Goethals, I. Van Driessche, F.J. Romero-Salguero, Chem. Soc. Rev. 42 (2013) 3913–3955.
[33] J. Ouwehand, J. Lauwaert, D. Esquivel, K. Hendrickx, V. Van Speybroeck, J.W. Thybaut, P. Van Der Voort, Eur. J. Inorg. Chem. 2016 (2016) 2144–2151.
[34] N. Zotova, A. Franzke, A. Armstrong, D.G. Blackmond, J. Am. Chem. Soc. 129 (2007) 15100–15101.
[35] S. Inagaki, S. Guan, T. Ohsuna, O. Terasaki, Nature 416 (2002) 304–307.